JOURNAL OF SOLID STATE CHEMISTRY 91, 131–139 (1991)

The Crystal Structure of a New Quaternary Ferrite: $Ba_{12}Fe_{28}Ti_{15}O_{84}$

IAN E. GREY,* ANDRÉ COLLOMB, AND XAVIER OBRADORS†

Laboratoire de Cristallographie, Centre National de la Recherche Scientifique, 166X, 38042 Grenoble Cedex, France

Received October 1, 1990

The quaternary ferrite $Ba_{12}Fe_{28}Ti_{15}O_{84}$ has monoclinic symmetry, space group $C2/m$, $a = 9.988(7)$, $b = 17.298(9)$, $c = 19.17(2)$ Å, $\beta = 99.33(6)°$, $Z = 2$. The crystal structure was refined to $R_w = 0.048$ for 2283 independent reflections collected on a Philips PW1100 diffractometer using Ag$K\alpha$ radiation. The structure is based on a close packed array of Ba + O atoms with a 24-layer stacking sequence $(cchcccch)_3$ along c^* and with metal atoms occupying both octahedral and tetrahedral interstices. The iron and titanium atoms are substantially ordered into blocks of cubic stacked layers centered at $z = 0$ and $\frac{1}{2}$, respectively. The titanium rich segments have a structure closely related to cubic $BaTiO_3$ while the iron rich blocks have features in common with the spinel structure. The two blocks are joined via a transition layer containing both titanium- and iron-rich octahedra.

Introduction

As part of an ongoing research program on the structures and magnetic properties of hexagonal ferrites (*1–5*) we surveyed (*6*) ternary diagrams involving oxides of tetravalent elements, $BaO–Fe_2O_3–MO_2$ (M = Sn, Ti). In the case of SnO_2 previous studies have revealed at least five different quaternary compounds (*7*) whereas for TiO_2 the R-type ferrite, $BaFe_4Ti_2O_{11}$, is the only reported compound (*8*). We attempted to grow single crystals of this phase for a study of its magnetic properties. Slow cooling in a KBO_2 flux (*6*) yielded a mixture of $BaFe_{12}O_{19}$ and large platy crystals of a strongly magnetic phase, subsequently shown by structure determination and microprobe analyses to have the composition $Ba_{12}Fe_{28}Ti_{15}O_{84}$. We describe here the determination and refinement of the structure of this new ferrite phase.

Experimental

Crystals of the new phase were obtained during an attempted preparation of $BaFe_4Ti_2O_{11}$ by the flux method. A 1 : 2 : 2 : 10 molar mixture of $BaCO_3$, Fe_2O_3, TiO_2, and KBO_2 was contained in a platinum crucible and held for 36 hr at 1573 K in air, then cooled to 1323 K at 3 K/hr. The crucible was then removed from the furnace and the flux dissolved in hot water. Shiny black crystals of the quaternary ferrite had a tabular or platy form with complex edge faceting. They were readily distinguished from crystals of $BaFe_{12}O_{19}$ by the way they stood on edge when placed near a hand magnet.

* Address for correspondence: CSIRO Division of Mineral Products, P.O. Box 124, Port Melbourne, Victoria 3207, Australia.

† Present address: Dept. Fisica Atomica y Nuclear, Facultad de Fisica, Universidad de Barcelona, Diagonal 645, Barcelona-28, Spain.

0022-4596/91 $3.00

Analyses were carried out on polished cross-sections of three crystals using a Cameca CAMEBAX electron probe microanalyzer operated at 20 kV and 50 nA. Standards used were $BaTiO_3$, Fe_2O_3, and TiO_2. A number of point analyses were made from rim to center on each of the crystals. There were no significant intra- or intergrain composition variations. The average of 15 analyses gave BaO 33.3(2)%, TiO_2 23.0(2)% and Fe_2O_3 42.5(3)%.

A powder X-ray diffraction pattern was obtained on ground crystals and found to be different from the reported patterns of the known barium titanates and barium ferrites. However, the strong peaks in the diffractogram could be indexed on a 4.08 Å, *I*-centered cubic subcell, analogous to that for cubic $BaTiO_3$. Precession photographs showed that most crystals were twinned. Studies on untwinned crystals showed them to have C-centered monoclinic symmetry, possible space groups *C*2/*m*, *C*2 or *Cm*, with approximate cell parameters $a \sim 10.0$, $b \sim 17.3$, $c \sim 19.2$ Å, $\beta \sim 99.3°$.

A tabular crystal measuring 0.066 × 0.090 × 0.140 mm was used for the collection of intensity data on a PW1100 diffractometer, using graphite monochromated Ag$K\alpha$ radiation ($\lambda = 0.56083$ Å). The crystallographic data are summarized in Table I. An ω-2θ scan was used for measurement of reflections ($\pm h$, k, $\pm l$) with $\sin\theta/\lambda < 0.60$ Å^{-1}. Double scans were used for reflections that did not acquire 2000 counts in the first scan. The intensities of two standard reflections were monitored every 2 hr. The intensity data were corrected for Lorentz and polarization effects and for absorption and reduced to 2283 independent structure amplitudes, with $R_{int} = 4.8\%$.

TABLE I

CRYSTALLOGRAPHIC DATA FOR $Ba_{12}Fe_{28}Ti_{15}O_{84}$

Space group	*C*2/*m*
Crystal size (mm)	0.066 × 0.090 × 0.140
a (Å)	9.988(7)
b (Å)	17.298(9)
c (Å)	19.17(2)
β(°)	99.33(6)
Z	2
Density (calc) (g/cm^3)	5.36
μ (Ag$K\alpha$) (cm^{-1})	78.3
Scan width of 2θ (°)	1.2 + 0.3 tan θ
Scan speed (°/min)	1.2
Number of independent reflections	2283
Final *R*	0.047
Final $R_w(w = 1/\sigma^2(F_o))$	0.048

The refinement of the structure was made using SHELX-76 (*9*). All values for X-ray scattering factors for neutral atoms and anomalous dispersion coefficients were taken from "International Tables for X-ray Crystallography" (*10*). Polyhedral structure diagrams were generated with STRUPLO (*11*).

Structure Determination and Refinement

As previously discussed by Tillmanns, Hofmeister, and Baur (*12*) for the case of barium titanates, routine methods for crystal-structure determination are generally unsuccessful for structures with low unit cell symmetry and high pseudosymmetry. They noted that the problem of distribution of a number of crystallographically independent large cations (Ba^{2+}) among the anion positions of a close-packed framework requires trial and error methods. "Only after exhaustive trials with different sets of assumptions based on experience with other barium titanate structures was it possible to derive from the Patterson synthesis a model of the crystal structure" (*12*). The structure of the new quaternary ferrite falls into this category. Direct methods and Patterson search methods were not successful.

The structure determination was assisted by noting the similarity of the unit cell symmetry and dimensions to those for $Ba_6Ti_{17}O_{40}$ (*13*). This suggested a related close-packed array of oxygen and barium atoms, having an eight-layer repeat (layers parallel to (001)) and 24 atoms per layer, with titanium and iron atoms occupying octahedral

(and perhaps tetrahedral) voids. On the assumption of no anion vacancies (subsequently verified from the structure solution) there are thus 192 oxygen plus barium atoms per unit cell. The microprobe analyses were used with this information to derive a starting unit cell composition of $Ba_{23}Fe_{56.5}Ti_{30.5}O_{169}$.

The approximate distribution of Ba + O or Fe, Ti in the eight anion and eight cation (001) layers was determined from an analysis of the (00l) reflections. An idealized close-packed geometry was used with the layers having z values that were multiples of $\frac{1}{16}$. A center of symmetry was assumed ($C2/m$). A single "atom" with the same scattering curve and isotropic displacement parameter was assigned to each layer. The occupancy factor for one layer was fixed and the F values of reflections (001) to (0023) were used to refine the occupancy factors of the other layers and the scale. These were then scaled by the unit cell composition to obtain an approximate measure of the number of electrons per layer. By this procedure it was established that the unit cell origin lay within a metal layer, and that the anion layers containing the highest density of barium atoms (6Ba + 18O) occurred at $z = \pm\frac{7}{16}$. It was also found that the refinement could be improved by introducing some atomic scattering halfway between some of the layers, indicating occupancy of some tetrahedral sites.

Starting with different ordering schemes of 6Ba + 18O in the layers at $z = \pm\frac{7}{16}$, a combination was eventually found that led to the location of the other metal atoms by Fourier methods. Refinement of all metal atoms using 998 reflections with $\sin\theta < 0.25$ gave an R factor of 19%. A difference Fourier map then revealed the positions of all oxygen atoms. Refinement of all coordinates, isotropic displacement parameters and Fe, Ti distributions using $1/\sigma^2$ weights, and all 2283 reflections resulted in convergence at $R = 0.047$, $R_w = 0.048$. The final refinement cycle involved 168 variables and the largest shift/error was 0.095 (y for Ba, for which the e.s.d. = 0.00005). The main peaks in the final difference Fourier map, 2–4 eA^{-2}, were all associated with the barium atom sites. The refined values of the atomic coordinates, isotropic displacement parameters, and Fe/Ti site occupancies are reported in Table II. The table of observed

TABLE II

COORDINATES AND ISOTROPIC THERMAL PARAMETERS FOR $Ba_{12}Fe_{28}Ti_{15}O_{84}$

Atom	Fraction Fe in M site	x	y	z	U (Å^2)
Ba(1)		0.3174(1)	0.1633(1)	0.4381(1)	0.0086(2)
Ba(2)		0.8076(1)	0	0.4405(1)	0.0101(3)
Ba(3)		0.4387(1)	0.3327(1)	0.3107(1)	0.0086(2)
Ba(4)		0.3152(1)	0	0.0839(1)	0.0122(3)
M(1)	1.0	0	0	0	0.0070(8)
M(2)	1.0	0.1714(2)	0.1720(1)	0.0272(1)	0.0060(4)
M(3)	0.91(6)	0	0.3442(2)	0	0.0062(10)
M(4)	0.83(6)	0.7039(3)	0	0.1112(2)	0.0071(10)
M(5)	0.87(4)	0.9520(2)	0.2583(1)	0.1327(1)	0.0060(7)
M(6)	0.91(5)	0.7097(2)	0.1644(1)	0.1332(1)	0.0068(7)
M(7)	0.88(4)	0.9835(2)	0.0858(1)	0.1335(1)	0.0062(7)
M(8)	0.68(6)	0.2697(3)	$\frac{1}{2}$	0.2594(2)	0.0085(11)
M(9)	0.24(4)	0.5098(2)	0.0927(1)	0.2502(1)	0.0072(8)
M(10)	0.33(6)	0.2368(3)	0	0.2519(2)	0.0084(11)
M(11)	0.58(5)	0.2396(2)	0.1762(1)	0.2487(1)	0.0090(8)
M(12)	0.37(5)	0.1370(2)	0.3250(1)	0.3803(1)	0.0094(8)
M(13)	0.30(6)	0.1132(3)	0	0.3807(2)	0.0089(12)
M(14)	1.0	0.4714(3)	0	0.4044(2)	0.0092(6)
M(15)	0.39(6)	0	0.1665(2)	$\frac{1}{2}$	0.0106(12)
O1		0.3054(3)	0	0.4331(7)	0.007(3)
O2		0.3168(9)	0.3322(5)	0.4373(5)	0.006(2)
O3		0.0626(9)	0.0830(5)	0.4385(5)	0.010(2)
O4		0.0658(9)	0.2493(5)	0.4378(5)	0.008(2)
O5		0.0681(9)	0.4108(5)	0.4322(5)	0.006(2)
O6		0.4530(10)	0.1683(5)	0.3111(5)	0.010(2)
O7		0.4342(14)	$\frac{1}{2}$	0.3199(7)	0.013(3)
O8		0.4397(12)	0	0.3045(6)	0.002(2)
O9		0.1832(9)	0.0796(5)	0.3113(5)	0.008(2)
O10		0.1987(10)	0.2428(5)	0.3191(5)	0.011(2)
O11		0.1893(9)	0.4126(5)	0.3104(5)	0.007(2)
O12		0.0620(9)	0.1711(5)	0.1896(5)	0.009(2)
O13		0.0597(9)	0.3377(5)	0.1824(5)	0.005(2)
O14		0.0792(13)	0	0.1837(7)	0.008(3)
O15		0.0777(13)	$\frac{1}{2}$	0.1961(7)	0.008(3)
O16		0.3186(9)	0.0857(5)	0.2024(5)	0.007(2)
O17		0.3092(10)	0.2520(5)	0.1899(5)	0.009(2)
O18		0.3137(9)	0.4218(5)	0.1839(5)	0.007(2)
O19		0.3558(9)	0.1675(5)	0.0597(5)	0.007(2)
O20		0.3641(9)	0.3305(5)	0.0743(4)	0.002(2)
O21		0.3762(15)	$\frac{1}{2}$	0.0714(7)	0.014(3)
O22		0.1009(9)	0.0814(5)	0.0599(5)	0.008(2)
O23		0.0978(9)	0.2594(5)	0.0659(5)	0.008(2)
O24		0.1090(10)	0.4175(5)	0.0605(5)	0.010(2)

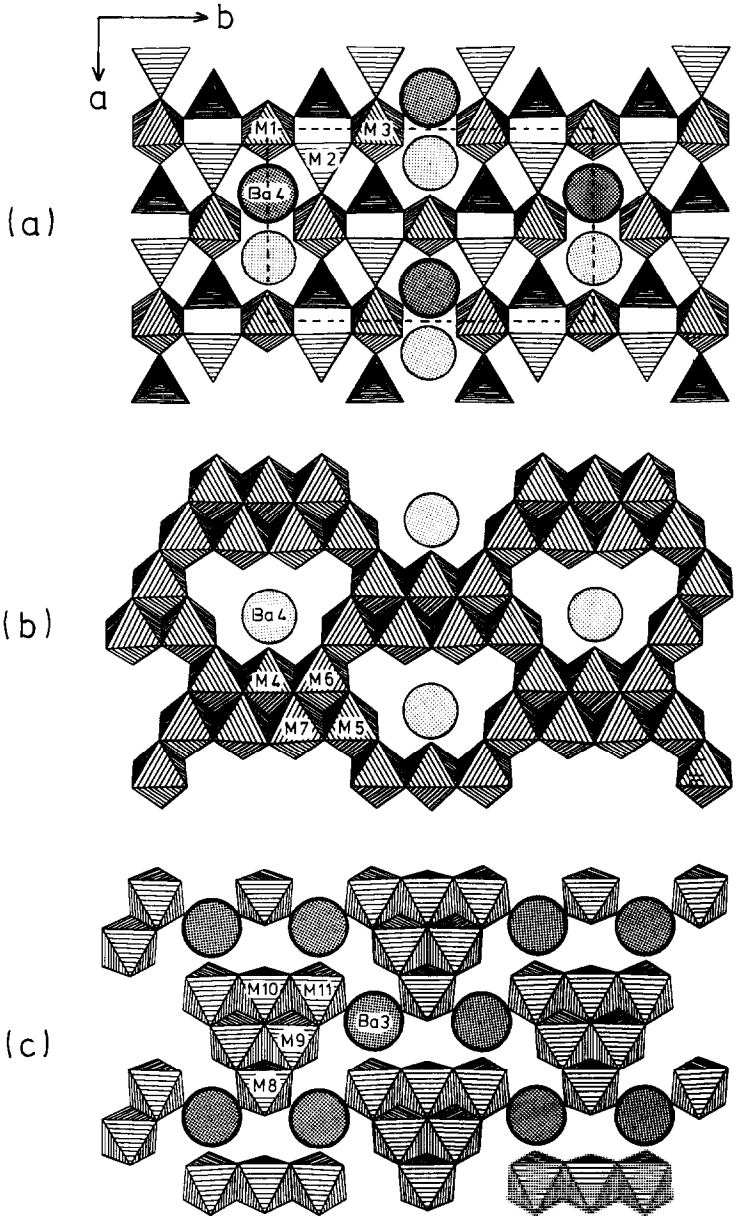

FIG. 1. Representation of (00l) polyhedral layers centered on metals at $z = 0$ (a), $z = \frac{1}{8}$ (b), $z = \frac{1}{4}$ (c), $z = \frac{3}{8}$ (d), and $z = \frac{1}{2}$ (e). Barium atoms in upper and lower anion layers represented by heavy and light shaded circles. Projection along c^*

and calculated Fs can be obtained from the authors.

The difficulty in solving a structure of this type is illustrated by the results below for R factors obtained when the barium atoms are introduced one at a time into the structure model. The final refined coordinates for the barium atoms were used in conjunction with all reflections with $\sin\theta <$ 0.25.

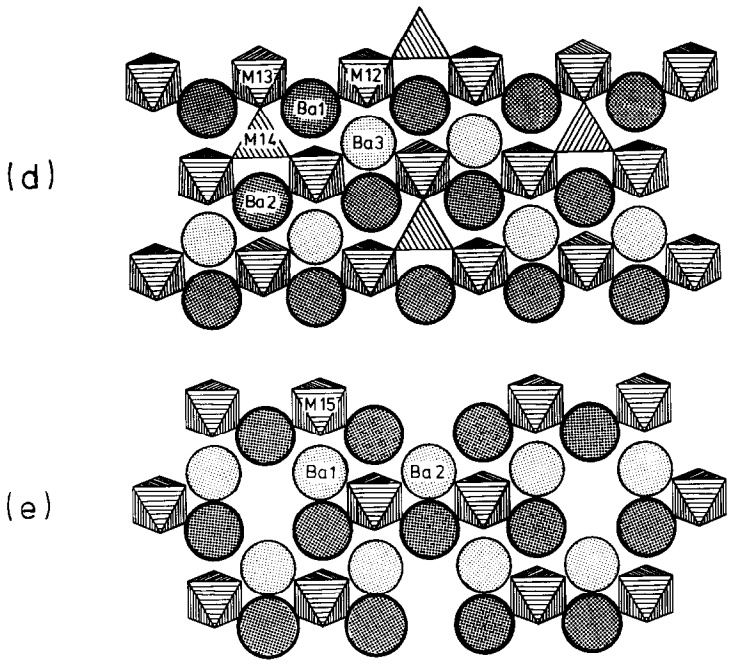

FIG. 1—*Continued*

Ba(1)	$R = 0.56$
Ba(1) + Ba(2)	$R = 0.57$
Ba(1) + Ba(2) + Ba(3)	$R = 0.56$
Ba(1) + Ba(2) + Ba(3) + Ba(4)	$R = 0.55$.

Description and Discussion of the Structure

The unit cell composition obtained from the structure refinement is $Ba_{24}M_{86}O_{168}$. On the basis that the iron is in the ferric form, charge balance is achieved with M = 56Fe + 30Ti, giving a unit cell formula of $Ba_{24}Fe_{56}Ti_{30}O_{168}$ which compares closely with the formula obtained from the microprobe analyses. Reasonable agreement is also obtained with the results of the cation site occupancy refinements (see Table II), $Ba_{24}Fe_{58.6}Ti_{27.4}O_{168}$.

The structure of $Ba_{12}Fe_{28}Ti_{15}O_{84}$ is based on a close packing of barium and oxygen atoms, with iron and titanium atoms occupying both octahedral and tetrahedral interstices. The closest-packed layers are parallel to (001) and have a 24-layer stacking sequence ABCBACBABCACBACBCAB ACBACA along c^*, or $(cchcccch)_3$. Each unit cell layer contains 24 Ba + O; there are no anion vacancies as in some barium titanates (*13*). There are four crystallographically distinct layer types, containing 0, 2, 4, and 6 barium atoms. The layer comprising exclusively oxygens, at $z \sim 0.31$, has h stacking of adjacent layers whereas the three layers containing both barium and oxygen atoms each have c stacking of the adjacent layers.

The ordering of iron and titanium atoms into octahedral and tetrahedral voids in the close-packed anion array gives rise to five crystallographically independent metal atom layers which are illustrated in Fig. 1 (a–e). The metal atom arrangement is of a beautiful and complex kind, and quite dif-

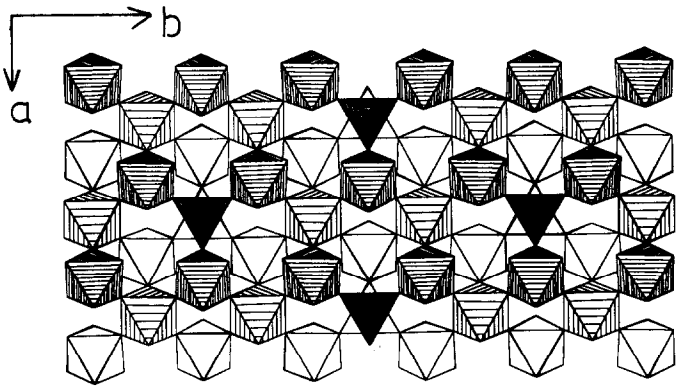

FIG. 2. Polyhedral articulation between cubic perovskite-like layers. Octahedra centered at $z = \frac{5}{8}$ and $\frac{1}{2}$ and $\frac{3}{8}$ are shown by heavy, medium, and no shading, respectively.

ferent to that in other barium titanates and ferrites. The most readily identifiable feature of the structure is a cubic perovskite-like block, four anion layers thick, centered at $z = \frac{1}{2}$. The interlayer polyhedra articulation for this block is illustrated in Fig. 2. The perovskite-like framework of corner-shared octahedra is modified by the replacement of one-third of the octahedra in the central layer by a pair of tetrahedra in the adjacent layers, situated above and below the empty octahedral site. There is a corresponding replacement of one-third of the barium atoms in the outermost anion layers of the block by oxygen atoms at the vertex of each tetrahedron.

A second identifiable structure element is a cubic spinel-related metal atom layer at $z = 0$. This is analogous to the mixed octahedral/tetrahedral (111) layer in spinel, except for the ordered omission of one-third of the tetrahedra. The vertex oxygen of the empty tetrahedral sites is replaced by barium. The articulation of the octahedra and tetrahedra at $z = 0$ to octahedra in the adjacent layers is also the same as that in spinel. This is illustrated in Fig. 3.

The linking of the two cubic stacked

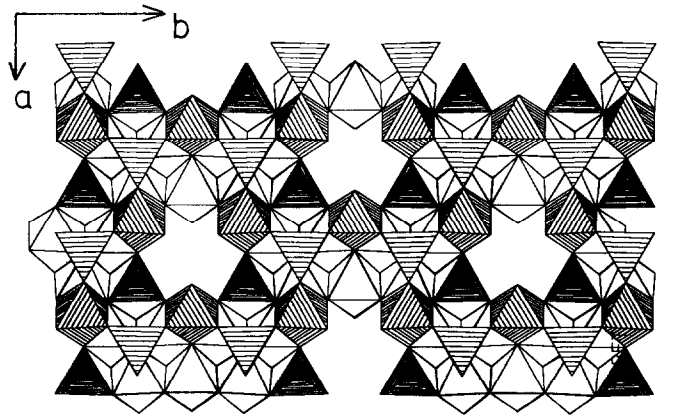

FIG. 3. Polyhedral articulation between spinel-related layers centered at $z = -\frac{1}{8}$ (light shading) and $z = 0$ (heavy shading).

structure blocks centered at $z = 0$ and $\frac{1}{2}$ is via the metal atom layer at $z = \frac{1}{4}$, illustrated in Fig. 1c, comprising islands of six edge-shared octahedra. This layer links to the spinel-like block via a hexagonally stacked oxygen-only layer, across which pairs of octahedra, $M(4)$ and $M(8)$, share a common face. Its linking to the perovskite-like block is via a cubic stacked layer of 4Ba + 20O. The octahedra share both corners and edges across this layer.

The results of the site occupancy refinements in Table II show that a high degree of ordering of titanium and iron occurs, with titanium dominant in the octahedra of the perovskite-like block and iron dominant in the spinel-like block. The intermediate layer at $z = \frac{1}{4}$ contains a mixture of titanium-rich and iron-rich octahedral sites. Thus in a general sense the structure is an intergrowth of blocks of cubic perovskite-related barium titanate and cubic barium ferrite separated by a transition layer of ferric titanate.

The bond lengths associated with the various polyhedra are reported in Table III. The mean Ba–O distance is similar for each of the four barium atoms, 2.889 to 2.993 Å. All four barium atoms lie in cubic stacked anion layers and thus have the same nearest neighbor cuboctahedral coordination. The individual Ba–O distances, 2.76 to 3.44, are within the range observed in other barium titanates and ferrites.

The M–O mean octahedral and tetrahedral distances are generally typical of those for close-packed structures containing iron and titanium, e.g., $BaFe_4Ti_2O_{11}$ (*14*) and $BaFe_{12}O_{19}$ (*1*). A notable exception is $M(15)$, Fig. 1e, which is located in the center of the perovskite block. This octahedral site has the ideal cubic perovskite environment with corner sharing of all six vertices with other octahedra and with a cube of eight barium atoms as second nearest neighbors. The site is occupied predominantly by titanium and has very little distortion of the octahedral geometry. The mean $M(15)$–O of 2.03 Å is very large, even allowing for some replacement by iron. In the parent structure, $BaTiO_3$, the valence requirements of the titanium are satisfied by an off-center displacement of the titanium atom, giving rise to ferroelectric behavior. However, there is no indication of this in $Ba_{12}Fe_{28}Ti_{15}O_{84}$. The isotropic displacement factor for $M(15)$ is normal and a refinement of anisotropic parameters showed no significant deviation from isotropic behavior. A related situation occurs for the tetrahedral Al atom in the center of the spinel block of β-alumina and magnetoplumbite structures. In these cases the anomalously long Al–O bonds are proposed to be a result of Al . . . Al nonbonded interactions (*15*). However, this is unlikely to be the explanation for the long $M(15)$–O bonds because the closest approach of surrounding M atoms is 3.96 Å. A similarly large average M–O distance of 2.04 Å has been reported for $M(1)$ in $BaFe_4Ti_2O_{11}$ (*14*) where the cation occupation of $M(1)$ has been determined from neutron diffraction refinements to be 0.45Ti(4+) + 0.55Fe(3+).

The shortest M–M distance is that between $M(4)$ and $M(8)$, 2.81 Å. These two octahedra, which contain predominantly iron, share a common face across the hexagonally stacked oxygen layer at $z \sim \frac{3}{16}$. However many of the M–M distances across shared octahedral edges are almost as short, 2.87–2.97 Å, see Table III.

It is interesting to note that the observation that $Ba_{12}Fe_{28}Ti_{15}O_{84}$ has the same-sized C-centered monoclinic cell as $Ba_6Ti_{17}O_{40}$ was used to help determine the structure, yet the two structures have almost nothing in common. The anion layer stacking sequences are different, $(cchcccch)_3$ and $(cchh)_6$, respectively, and the anion layers in $Ba_6Ti_{17}O_{40}$ contain vacancies. The barium titanate does not contain perovskite-like blocks as occurs in the titanium-rich segments of the barium iron titanate. The

TABLE III

INTERATOMIC DISTANCES (Å) IN $Ba_{12}Fe_{28}Ti_{15}O_{84}$

M(1) octahedron			*M*(2) tetrahedron			*M*(15) octahedron		
M(1)–O(22)	(×4)	1.985(9)	*M*(2)–O(19)		1.848(9)	*M*(15)–O(2)	(×2)	2.019(8)
M(1)–O(21)	(×2)	1.99(1)	*M*(2)–O(22)		1.869(9)	*M*(15)–O(3)	(×2)	2.03(1)
			M(2)–O(23)		1.886(9)	*M*(15)–O(4)	(×2)	2.04(1)
			M(2)–O(20)		1.920(8)			
M(3) octahedron			*M*(4) octahedron			Ba(1) polyhedron		
M(3)–O(24)	(×2)	1.930(9)	*M*(4)–O(24)	(×2)	1.892(9)	Ba(1)–O(10)		2.760(9)
M(3)–O(19)	(×2)	1.99(1)	*M*(4)–O(21)		1.99(1)	Ba(1)–O(1)		2.829(2)
M(3)–O(23)	(×2)	2.073(9)	*M*(4)–O(18)	(×2)	2.116(9)	Ba(1)–O(5)		2.833(9)
			M(4)–O(15)		2.22(1)	Ba(1)–O(5)		2.864(9)
M(5) octahedron			*M*(6) octahedron			Ba(1)–O(4)		2.898(9)
M(5)–O(13)		1.902(9)	*M*(6)–O(13)		1.90(1)	Ba(1)–O(3)		2.902(9)
M(5)–O(17)		1.95(1)	*M*(6)–O(17)		1.977(9)	Ba(1)–O(4)		2.908(9)
M(5)–O(20)		2.016(8)	*M*(6)–O(18)		1.979(9)	Ba(1)–O(4)		2.921(9)
M(5)–O(19)		2.022(9)	*M*(6)–O(23)		2.045(9)	Ba(1)–O(2)		2.923(9)
M(5)–O(12)		2.069(9)	*M*(6)–O(20)		2.058(9)	Ba(1)–O(2)		2.93(1)
M(5)–O(23)		2.09(1)	*M*(6)–O(24)		2.122(9)	Ba(1)–O(9)		2.956(9)
						Ba(1)–O(6)		2.97(1)
M(7) octahedron			*M*(8) octahedron					
M(7)–O(12)		1.917(9)	*M*(8)–O(7)		1.85(1)			
M(7)–O(14)		1.935(8)	*M*(8)–O(11)	(×2)	2.04(1)	Ba(3) polyhedron		
M(7)–O(22)		1.98(1)	*M*(8)–O(18)	(×2)	2.08(1)	Ba(3)–O(12)		2.80(1)
M(7)–O(21)		2.086(9)	*M*(8)–O(15)		2.09(1)	Ba(3)–O(17)		2.829(9)
M(7)–O(20)		2.089(8)				Ba(3)–O(6)		2.848(9)
M(7)–O(18)		2.09(1)				Ba(3)–O(11)		2.849(9)
						Ba(3)–O(9)		2.875(9)
M(9) octahedron			*M*(10) octahedron			Ba(3)–O(10)		2.885(9)
M(9)–O(13)		1.90(1)	*M*(10)–O(14)		1.87(1)	Ba(3)–O(2)		2.89(1)
M(9)–O(6)		1.90(1)	*M*(10)–O(9)	(×2)	1.92(1)	Ba(3)–O(10)		2.89(1)
M(9)–O(11)		1.970(9)	*M*(10)–O(16)	(×2)	2.01(1)	Ba(3)–O(7)		2.901(2)
M(9)–O(16)		1.983(9)	*M*(10)–O(8)		2.11(1)	Ba(3)–O(4)		2.924(9)
M(9)–O(15)		2.083(9)				Ba(3)–O(3)		2.944(9)
M(9)–O(8)		2.094(8)				Ba(3)–O(18)		2.975(9)
M(11) octahedron			*M*(12) octahedron					
M(11)–O(10)		1.87(1)	*M*(12)–O(4)		1.92(1)			
M(11)–O(17)		1.93(1)	*M*(12)–O(2)		1.948(9)			
M(11)–O(12)		1.945(9)	*M*(12)–O(5)		1.973(9)			
M(11)–O(16)		2.023(9)	*M*(12)–O(10)		2.00(1)			
M(11)–O(9)		2.185(9)	*M*(12)–O(6)		2.087(9)			
M(11)–O(6)		2.272(9)	*M*(12)–O(11)		2.14(1)			
M(13) octahedron			*M*(14) tetrahedron					
M(13)–O(3)	(×2)	1.93(1)	*M*(14)–O(1)		1.83(1)			
M(13)–O(7)		1.97(1)	*M*(14)–O(5)	(×2)	1.852(9)			
M(13)–O(1)		2.02(1)	*M*(14)–O(8)		1.89(1)			
M(13)–O(9)	(×2)	2.11(1)						

Ba(2) polyhedron		
Ba(2)–O(7)		2.81(1)
Ba(2)–O(5)	(×2)	2.830(9)
Ba(2)–O(1)		2.84(1)
Ba(2)–O(3)	(×2)	2.853(9)
Ba(2)–O(2)	(×2)	2.906(9)
Ba(2)–O(3)	(×2)	2.931(9)
Ba(2)–O(11)	(×2)	2.990(9)

Ba(4) polyhedron		
Ba(4)–O(16)	(×2)	2.78(1)
Ba(4)–O(22)	(×2)	2.842(9)
Ba(4)–O(22)		2.86(1)
Ba(4)–O(12)	(×2)	2.937(9)
Ba(4)–O(24)	(×2)	3.04(1)
Ba(4)–O(24)	(×2)	3.20(1)
Ba(4)–O(21)		3.44(1)

Shortest *M*–*M* distances:

M(1)–*M*(7)	2.986(3)	*M*(2)–*M*(7)	3.337(4)
M(3)–*M*(6)	3.032(3)	*M*(4)–*M*(8)	2.810(6)
M(4)–*M*(6)	2.874(2)	*M*(5)–*M*(6)	2.899(3)
M(5)–*M*(3)	3.050(3)	*M*(5)–*M*(7)	3.000(3)
M(5)–*M*(6)	2.916(3)	*M*(7)–*M*(7)	2.968(4)
M(7)–*M*(4)	3.130(4)	*M*(7)–*M*(6)	3.053(3)
M(8)–*M*(9)	3.032(4)	*M*(9)–*M*(10)	3.168(4)
M(9)–*M*(12)	2.972(3)	*M*(10)–*M*(13)	2.934(6)
M(11)–*M*(10)	3.049(2)	*M*(11)–*M*(9)	3.057(3)
M(14)–*M*(10)	3.437(6)	*M*(15)–*M*(13)	3.955(4)

most prominent structural elements of $Ba_6Ti_{17}O_{40}$ are V_3O_5-type ribbons of edge-shared octahedra, which do not occur in the barium iron titanate. The iron-rich blocks also have no structural counterpart in the known barium ferrites. The response of single crystals to a hand magnet indicates that the magnetic moments on the iron atoms are aligned ferromagnetically within the (001) planes. Studies are under way to characterize the magnetic properties of $Ba_{12}Fe_{28}Ti_{15}O_{84}$.

Acknowledgments

We thank A. Durif and J. C. Guitel for help with the x-ray intensity data collection and processing, and Mr. J. A. Watts for his constructive criticism of this manuscript.

References

1. X. OBRADORS, A. COLLOMB, M. PERNET, D. SAMARAS, AND J. C. JOUBERT, *J. Solid State Chem.* **56,** 171 (1975).
2. X. OBRADORS, J. TEJADA, A. ISALGUE, A. COLLOMB, M. PERNET, AND J. C. JOUBERT, *Adv. Ceram.* **15,** 259 (1985).

3. A. COLLOMB, X. OBRADORS, A. ISALGUE, M. PERNET, AND J. C. JOUBERT, *Adv. Ceram.* **15,** 255 (1985).
4. A. COLLOMB, P. WOLFERS, AND X. OBRADORS, *J. Magn. Magn. Mater.* **62,** 57 (1986).
5. A. COLLOMB, M. A. HADJ FARHAT, AND J. C. JOUBERT, *Mater. Res. Bull.* **24,** 453 (1989).
6. X. OBRADORS, These de 3e cycle, Universite de Grenoble (1983).
7. M. C. CADEE AND D. J. W. IJDO, *J. Solid State Chem.* **36,** 314 (1981).
8. F. HABEREY AND M. VELICESCU, *Acta Crystallogr. Sect. B* **30,** 1507 (1974).
9. G. M. SHELDRICK, SHELX76. A program for crystal structure determination. Univ. of Cambridge, England (1976).
10. International Tables for X-Ray Crystallography, Vol. IV, Birmingham, Kynoch Press (1974).
11. R. X. FISCHER, STRUPLO'84. A Fortran plotprogram for crystal structure illustrations. Univ. of Wurzburg, FRG. (version of June, 1986).
12. E. TILLMANNS, W. HOFMEISTER, AND W. H. BAUR, *J. Amer. Ceram. Soc.* **66,** 268 (1983).
13. E. TILLMANNS AND W. H. BAUR, *Acta Crystallogr. Sect. B* **26,** 1645 (1970).
14. X. OBRADORS, A. COLLOMB, J. PANNETIER, A. ISALGUE, J. TEJADA, AND J. C. JOUBERT, *Mater. Res. Bull.* **18,** 1543 (1983).
15. T. R. WAGNER AND M. O'KEEFFE, *J. Solid State Chem.* **73,** 211 (1988).